Probing the mechanical properties of graphene using a corrugated elastic substrate

Scott Scharfenberg, D. Z. Rocklin, Cesar Chialvo, Richard L. Weaver, Paul M. Goldbart,[a] and Nadya Mason[b]

Department of Physics, University of Illinois at Urbana-Champaign, 1110 West Green Street, Urbana, Illinois 61801, USA

(Received 29 November 2010; accepted 19 January 2011; published online 1 March 2011)

We examine the mechanical properties of graphene samples of thicknesses ranging from 1 to 17 atomic layers, placed on a microscale-corrugated elastic substrate. Using atomic force microscopy, we show that the graphene adheres to the substrate surface and can substantially deform the substrate, with larger graphene thicknesses creating greater deformations. We use linear elasticity theory to model the deformations of the composite graphene-substrate system. We compare experiment and theory, and thereby extract information about graphene's bending rigidity, adhesion, critical stress for interlayer sliding, and sample-dependent tension. © *2011 American Institute of Physics*. [doi:10.1063/1.3553228]

The exceptional mechanical properties of graphene have made it attractive for nanomechanical devices and functional composite materials.[1] Elastic properties have been measured using nanoindentation[2] and pressurization[3] techniques, and Young's modulus E was found to be exceptionally high, ~1 TPa. Graphene's van der Waals adhesion to surfaces has been examined theoretically,[4] as has adhesion to nanoparticles.[5] However, it is typically difficult to extract experimental parameters for adhesion, despite the fact that these properties can strongly influence its electronic[6] and mechanical[7,8] behavior. In addition, the mechanical interplay between graphene and other materials has not been well studied, although it is crucial to the use of graphene in composite,[1] flexible, or strain-engineered[9] materials.

In this letter, we explore both elasticity and adhesion, as evident in the interaction between microscale-corrugated elastic substrates and few layer graphene (FLG). By using an atomic force microscope (AFM) to determine surface adhesion and deformations, we find that FLG can fully adhere to the corrugated substrate, and that thicker samples flatten the corrugated substrate more than thinner samples do. By developing a linear elasticity theory to model the flattening and adhesion as functions of layer thickness, we are able to extract information about graphene's bending rigidity, adhesion, critical stress for interlayer sliding, and sample-dependent tension.

Sample substrates were prepared by casting a 3 mm thick layer of polydimethylsiloxane (PDMS)—which cures into a flexible rubbery material—onto the exposed corrugated surface of a writable compact disk. This resulted in approximately sinusoidal corrugations on the PDMS, having a wavelength of 1.5 μm and a depth of 200 nm [see Fig. 1(a)]. Graphene was then deposited onto the PDMS via mechanical exfoliation.[10] Samples were imaged on an Asylum Research MFP-3D AFM. Figure 1(a) shows a topographic image of FLG on the PDMS; it is evident from the image that the graphene conforms to the corrugations [Fig. 1(b)].

In order to fit the experimental data to a theoretical model, it was necessary to determine (1) the thickness of the FLG, (2) the conformation between the FLG and the PDMS, and (3) the height profiles. The soft substrate created difficulty in measuring FLG thickness via established AFM and Raman techniques. Thus, the thickness was determined by using the AFM (in contact mode) to fold the flake onto itself (once all other measurements were completed), and then using the AFM again to measure the resultant FLG-FLG step height. An example of AFM-folded FLG is shown in Fig. 2(a).

The areas of the graphene that adhered to the PDMS were identified by measuring the phase of the oscillation of the AFM cantilever. This phase is determined by the electrostatic properties of the surface; sections having the same ad-

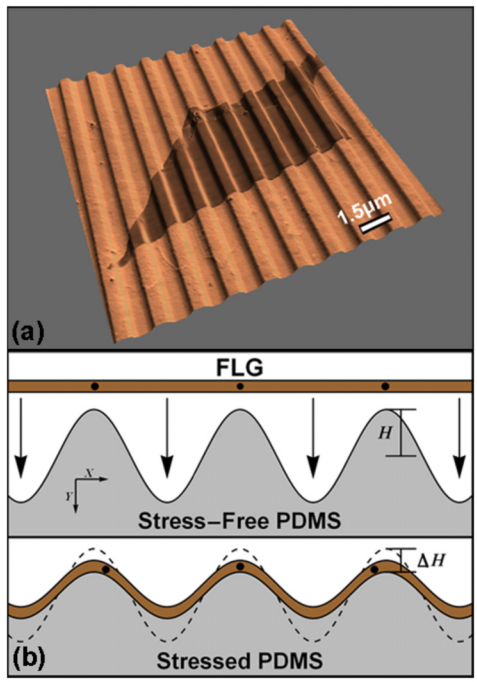

FIG. 1. (Color online) (a) AFM topographic image of FLG on corrugated PDMS (AFM height and phase data superimposed). (b) Illustration of FLG-PDMS interaction, showing how FLG adheres to and flattens the PDMS corrugations.

[a]Present address: School of Physics, Georgia Institute of Technology, 837 State Street, Atlanta, GA 30332-0430.
[b]Electronic mail: nadya@illinois.edu.

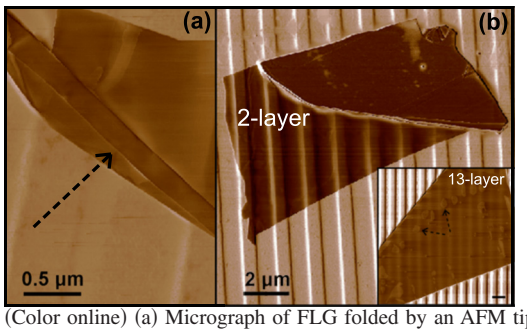

FIG. 2. (Color online) (a) Micrograph of FLG folded by an AFM tip, used for FLG thickness measurements. Dashed arrow shows direction AFM tip was dragged. (b) AFM phase images of FLG on PDMS. Main figure: flake of FLG, where the lower-left section is two-layer (upper right is much thicker, >100 layers). The two-layer region shows uniform adhesion over plateaus and valleys, indicated by homogeneous contrast over them. Inset: 13-layer graphene; bubblelike lighter patches (see dashed arrows) indicate inhomogeneous phase and adhesion.

hesion have common electrostatic properties and thus a common phase. The main image of Fig. 2(b) shows a two-dimensional phase map for two-layer FLG, in which the phase is uniform across the sample (except where adhesion is lost at the steepest slopes of the corrugation). These data demonstrate the near-conformal adhesion between the FLG and the PDMS and are consistent with previous work on graphene placed over more shallow depressions.[8] The AFM height data similarly indicate that the FLG adheres to the corrugations of the PDMS (e.g., see Fig. 3). In contrast, the inset to Fig. 2(b) shows the phase data for 13-layer FLG, where a bubblelike structure appears across the sample, showing that the phase is not uniform and, hence, that the FLG does not adhere well to the PDMS. In general, we found that samples having more than ~11 layers did not fully adhere; this is consistent with the predicted "snap-through" instability in graphene on a corrugated substrate.[11] The adhesive properties did not seem to depend on the size or aspect ratio of the graphene samples, only on their thickness.

Remarkably, interplay between the rigidity of the graphene and the shear modulus of the PDMS causes the FLG to become corrugated and the PDMS to be flattened. Figures 3(a) and 3(b) show image and height measurements for 8- and 13-layer cases, respectively. In Fig. 3(a) it is clear that the FLG maintains the basic shape of the PDMS corrugations, but pulls the corrugations up in the valleys and pushes them down on the plateaus. In contrast, Fig. 3(b) shows that the 13-layer FLG sits on top of the PDMS. Figure 4 shows the fractional height difference between the FLG-PDMS composite and the bare PDMS (the "flattening factor"), plotted against graphene thickness, for 18 samples (measured on nine different PDMS substrates). The amount of flattening increases with layer number.

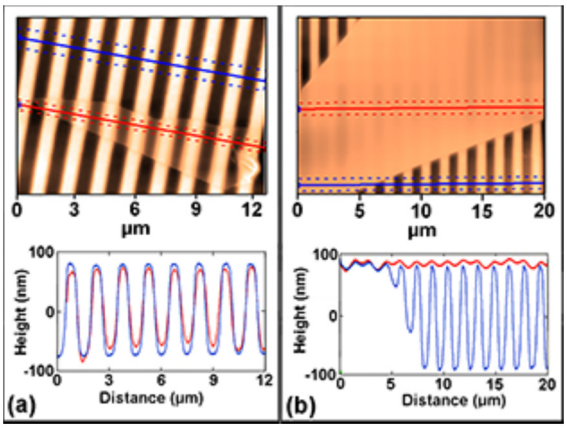

FIG. 3. (Color online) Image (top) and height measurements (bottom) for (a) eight-layer and (b) 13-layer graphene. Lines show trajectories of scans over FLG and PDMS. The 13-layer FLG is likely wavy due to slight sidewall adhesion.

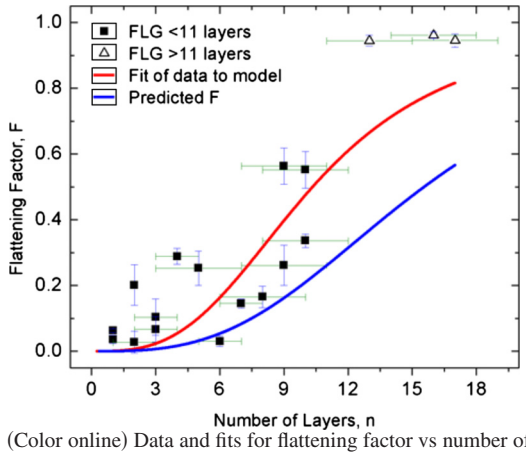

FIG. 4. (Color online) Data and fits for flattening factor vs number of layers. Symbols show measured flattenings. Samples with thicknesses >11 layers are shown with open triangles, as AFM height measurements are likely modified by the lack of adhesion to the substrate. Error bars are related to uncertainty in number of layers and spatial nonuniformity of flattening. Upper curve is least-squares fit to model, assuming zero tension in samples. Lower curve is predicted flattening for samples having zero tension (see text).

We now develop a linear elasticity theory, related to that of Yu and Suo,[12] in which we determine the surface stress required on both the initially flat (ignoring the nanometer-scale intrinsic ripples) FLG and the initially corrugated PDMS, such that they each deform to accommodate the other. Continuum models have been applied previously to characterize the bending rigidity of few-layer graphene.[14]

We consider an undeformed PDMS substrate having a corrugated surface: $h(x)=H\cos kx$ [see Fig. 1(b)]. Graphene adheres to and flattens this surface, reducing the corrugation amplitude. The normal stress $S\cos kx$ required to deform the graphene in this way then follows from thin plate theory.[13] An equal and opposite stress acts on the PDMS substrate, which we treat as semi-infinite, isotropic and incompressible. The shared profile of the distorted graphene and PDMS is determined by linear elastic theory, resulting in a fractional decrease in the amplitude of the PDMS corrugations, the *flattening factor*,

$$F \equiv \frac{\Delta H}{H} = \frac{(Mk^3/2\mu)}{1+(Mk^3/2\mu)}, \tag{1}$$

where ΔH is the change in the height of the corrugations resulting from application of the FLG, M is the flexural, or *bending*, rigidity and μ the PDMS shear modulus.

We now compare the model to the data to elucidate FLG's mechanical behavior. Figure 4 shows measured values of F versus n, along with a least-squares fit to Eq. (1) (upper curve), in which we assume M to be proportional to the cube of the number of layers, consistent with a continuum model for thick grapheme.[14] From the fit we extract a dimensionless graphene rigidity parameter $G \equiv Mk^3/2\mu n^3 = 0.000\,91$.

The shear modulus μ of PDMS was measured by nanoindentation to be $\mu=0.4$ MPa. Using $k=4.2\ \mu m^{-1}$, the bending rigidity of n-layer FLG is then obtained as $M=9.8\times10^{-18}n^3$ N m. This value is higher than that predicted using Kirchhoff plate theory, from which $M=E(nt)^3/12(1-\nu^2)=2.9\times10^{-18}n^3$ N m, using the graphene Young's modulus $E\approx900$ GPa,[15] Poisson ratio $\nu\approx0$, and per-layer thickness $t=0.335$ nm.[15] The predicted values for F are plotted as the lower curve in Fig. 3.

The spread in the data is greater than can be accounted for by measurement uncertainty. This leads us to hypothesize that the discrepancy between extracted and predicted values of F (or M) is caused by tension in the graphene. Because of its high stiffness against stretching we believe that as the FLG is applied to the substrate it slips until sample-dependent friction halts the process, leaving some tension in the FLG [see dots in Fig. 1(b)]. A tension T could modify the flattening factor in Eq. (1), giving

$$F \equiv \frac{\Delta H}{H_0} = \frac{(Mk^3/2\mu)+(Tk/2\mu)}{1+(Mk^3/2\mu)+(Tk/2\mu)}. \tag{2}$$

If we assume that the difference between the predicted values of F (lower curve) and the data in Fig. 4 is due to tension, we can use Eq. (2) to extract a value of tension for each sample. This yields tension values between 0 and 0.20 N m^{-1}, with no discernible trend with thickness. The maximum tension corresponds to a maximum axial strain of $T/ntE=7.8\times10^{-5}$. We can also use the tension to estimate the magnitude of the stress due friction: Assuming that the friction acts over a distance $d\geq10\ \mu$m, we find a stress T/d of less than 2×10^4 Pa. The condition that tension is positive, taken together with our data, implies that FLG's bending rigidity is not greater than $(1.6\pm0.8)n^3\times10^{-18}$ N m, similar to predicted values. If, as seems reasonable, the tension is negligibly small for at least one sample, then this bound would become an estimate of the graphene rigidity.

The data shown in Fig. 4 can also be used to estimate the normal interface stress $S=2\mu kFH$, which ranges from 1.1×10^5 to 3.0×10^5 Pa. The data also show that no samples which adhere to the surface have $F>0.6$, implying that the adhesive strength between the graphene and the PDMS is $\leq3.0\times10^5$ Pa. This inference is model-independent.

We can extract bounds on the graphene-PDMS adhesion energy by considering that the energy of the adhesion must be at least as large as the spatially averaged elastic deformation energy, E. E can be regarded as a sum of the elastic deformation of the substrate, the FLG deformation under tension, and the FLG bending. Ignoring the negligible tension contribution, the spatial average of these sums to $\mu kFH^2/2$. The maximum elastic energy (which is also the lower bound of the adhesive energy) in our samples is thus 0.044 eV/nm^2. This is consistent with the theoretical prediction of 0.04 eV/nm^2 for the van der Waals adhesive energy between graphene and a SiO_2 substrate.[4] Absent other significant contributions to the energy budget (such as work done against friction), the adhesion energy must equal the elastic energy and 0.044 eV/nm^2 becomes an estimate of the adhesive energy.

Even though thin plates have bending rigidity determined entirely by Young's modulus and thickness, there are nevertheless (small) shear strains developed interior to the plate (negligible in estimating bending rigidity). There are in consequence shear stresses developed within the graphene slab that are opposed by interlayer shear strength. These stresses could cause the graphene layers to slide relative to one another. In this case, the impact on the flattening factor is to modify the dependence of the bending rigidity on the number of layers from n^3 for a cohesive sample to $\Sigma_a n_a^3$, where n_a is the number of layers in the ath slab. We find that such a model does not improve the fits to the data, and thus find no evidence that the graphene layers slide. The physical effect of sliding would be to decrease the flattening factor, and thus sliding cannot explain the discrepancy between the theoretical values and data of Fig. 4. We hypothesize that there does, however, exist some critical shear stress beyond which layers slide relative to one another. Considering the finite thickness of the FLG, Mindlin plate theory[16] shows that the boundary stress needed to deform the FLG generates a central shear strain ϵ of

$$\epsilon = n^2t^2k^3(H-\Delta H)/4. \tag{3}$$

The absence of evidence for sliding in samples of <11 layers thus suggests a lower bound on the critical shear strain ϵ_{crit} of $\geq1.2\times10^{-5}$. Multiplying by the graphene shear modulus, which we take to be half its Young's modulus, this implies an interlayer shear strength ≥5.6 MPa.

To conclude, we have developed a method of measuring the mechanical properties of graphene using deformable microcorrugated substrates. We are able to put bounds on—or extract estimates for—fundamental properties such as graphene's bending rigidity, critical shear stress, and the FLG-PDMS adhesive strength and energy. We also extracted sample-dependent properties such as the tension and tangential interface stress. The experimental and theoretical techniques developed in this letter may be readily extended to various substrates having a range of surface geometries.

We thank Scott MacLaren (UIUC CMM) and Richard Nay (Hysitron) for technical assistance. This work was supported by DOE Grant No. DE-FG02-07ER46453, NSF Grant No. DMR06-44674, NSF Grant No. DMR09-06780, and an NDSEG Fellowship (D.Z.R.).

[1]See, e.g., A. K. Geim, Science **324**, 1530 (2009).
[2]C. Lee, X. Wei, J. W. Kysar, and J. Hone, Science **321**, 385 (2008).
[3]J. S. Bunch, S. S. Verbridge, J. S. Alden, A. M. V. D. Zande, J. M. Parpia, H. G. Craighead, and P. L. McEuen, Nano Lett. **8**, 2458 (2008).
[4]J. Sabio, C. Seoanez, S. Fratini, F. Guinea, A. H. Castro Neto, and F. Sols, Phys. Rev. B **77**, 195409 (2008).
[5]Z. Zong, C. Chen, M. R. Dokmeci, and K. Wan, J. Appl. Phys. **107**, 026104 (2010).
[6]X. Du, I. Skachko, A. Barker, and E. Y. Andrei, Nat. Nanotechnol. **3**, 491 (2008).
[7]J. S. Bunch, A. M. van der Zande, S. S. Verbridge, I. W. Frank, D. M. Tanenbaum, J. M. Parpia, H. G. Craighead, and P. L. McEuen, Science **315**, 490 (2007).
[8]C. Metzger, S. Remi, M. Liu, S. V. Kusminskiy, A. H. Castro Neto, A. K. Swan, and B. B. Goldberg, Nano Lett. **10**, 6 (2010).
[9]F. Guinea, M. I. Katsnelson, and A. K. Geim, Nat. Phys. **6**, 30 (2010).
[10]K. S. Novoselov, A. K. Geim, S. V. Morozov, D. Jiang, Y. Zhang, S. V. Dubonos, I. V. Grigorieva, and A. A. Firsov, Science **306**, 666 (2004).
[11]T. Li and Z. Zhang, Nanoscale Res. Lett. **5**, 169 (2010).
[12]H. H. Yu and Z. Suo, J. Mech. Phys. Solids **46**, 829 (1998).
[13]See, e.g., L. D. Landau and E. M. Lifshitz, *Theory of Elasticity*, Course of Theoretical Physics Vol. 7 (Pergamon, Oxford, 1986), Secs. 11 and 12.
[14]M. Poot and H. S. J. van der Zant, Appl. Phys. Lett. **92**, 063111 (2008).
[15]B. T. Kelly, *Physics of Graphite* (Applied Science, London, 1981).
[16]R. D. Mindlin, J. Appl. Mech. **18**, 31 (1951).